ARTICLE

Journal of Materials Chemistry
www.rsc.org/materials

Covalent modification of vapour-grown carbon nanofibers *via* direct Friedel–Crafts acylation in polyphosphoric acid

Jong-Beom Baek,[a,c] Christopher B. Lyons[b] and Loon-Seng Tan*[d]

[a]*University of Dayton Research Institute, 300 College Park, Dayton, OH, 45469-0168, USA*
[b]*Southwestern Ohio Council for Higher Education, 3155 Research Bldv., Suite 204, Dayton, OH, 45420-4015, USA*
[c]*School of Chemical Engineering, Chungbuk National University, Cheongju, Chungbuk, 361-763, South Korea*
[d]*Polymer Branch, Materials & Manufacturing Directorate, Air Force Research Laboratory, AFRL/MLBP, Wright-Patterson Air Force Base, Dayton, OH, 45433-7750, USA. E-mail: Loon-Seng.Tan@wpafb.af.mil*

Received 29th January 2004, Accepted 22nd April 2004
First published as an Advance Article on the web 19th May 2004

Electrophilic functionalization of vapour-grown carbon nanofibers (VGCNF) was accomplished *via* Friedel–Crafts acylation with 2,4,6-trimethylphenoxybenzoic acid in polyphosphoric acid using the improved conditions that we previously described. The progress of the reaction was conveniently monitored with FT-IR spectroscopy following the growth of the keto-carbonyl band at 1664 cm^{-1} associated with the product. In addition to scanning electron microscopic and UV-vis spectroscopic data, the combined results from the elemental analysis and thermogravimetric analysis further suggested that there were 3 arylcarbonyl groups covalently attached to the nanotube structure for every 100 carbon sites. Because of the presence of significant hydrogen content in the starting VGCNF, the covalent attachment of the arylcarbonyl groups most probably occurred at the sp^2C–H sites.

DOI: 10.1039/b401401d

1. Introduction

One-dimensional, carbon-based, nano-structured materials are generally divided into three categories based on their diameter dimensions: (i) single-wall carbon nanotubes or SWNTs (0.7–3 nm); (ii) multi-wall carbon nanotubes or MWNTs (2–20 nm); carbon nanofibers or CNFs (40–100 nm).[1] Because of the extraordinary thermal, mechanical, and electrical properties predicted for carbon nanotubes,[2] as a class of advanced materials, they have captivated wide-spread attention in the advanced materials research community in recent years. To take advantage of their predicted properties, the principal approach to utilizing the carbon nanotubes reported in the literature focused on blending and composites processing.[3] For composites processing, uniform dispersion of reinforcing nanounits is critical to achieving the optimal properties and the use of anionic polyelectrolytes was found to be effective.[4] As an approach to achieving a good dispersion of SWNT in a high performance polymer, *in-situ* polymerization of rigid-rod poly(benzobisoxazole) with SWNT in polyphosphoric acid (PPA) at 190 °C has also been reported recently.[5] Additionally, great strides have been achieved in the functionalization of SWNT to impart solubility and provide more processing options.[6] Similarly to fullerene chemistry, the general nature of almost all chemical reactions utilized in CNT functionalization to date is compatible with the electron-deficient character of the carbon nanotubes. Recently, Prato *et al.* first reported the application of electrophilic addition reactions to chloroalkylate the sidewall of SWNT and subsequent O-acylation (esterification) of the SWNT-bound hydroxyl groups.[7] However, to our knowledge, the direct Friedel–Crafts acylation of nanofibers or nanotubes has never been reported before. Thus, in this paper, we describe such functionalization on vapor grown carbon nanofibers (VGCNF). For practical considerations such as lower cost, easier accessibility, and availability in large quantities, we selected VGCNF instead of carbon nanotubes in our initial effort.

2. Experimental

2a. Materials

All reagents and solvents were purchased from Aldrich Chemical Inc. and used as received, unless otherwise specified. Vapor grown carbon nanofibers (VGCNF) were obtained from Applied Science Inc., Cedarville, OH.[8]

2b. Instrumentation

Proton and carbon nuclear magnetic resonance (^1H NMR and ^{13}C NMR, 270 and 50 MHz respectively) spectra were obtained on a Jeol-270 spectrometer. Infrared (FT-IR) spectra were recorded on a Bruker IFS 28 Equinox Fourier transform spectrophotometer. Elemental analysis and mass spectral analysis were performed by the System Supports Branch, Air Force Research Lab, Wright-Patterson Air Force Base, Ohio. The melting points (m.p.) of all the compounds were determined on a Mel-Temp melting point apparatus and are uncorrected. Thermogravimetric analyses (TGA) were obtained in helium and air atmospheres with a heating rate of 10 °C min^{-1} using a TA Hi-Res TGA 2950 thermogravimetric analyzer. The scanning electron microscope (SEM) used in this work is a Hitachi S-5200. UV-vis spectra were recorded on a Hewlett-Packard 8453 UV-visible spectrophotometer.

2c. 4-(2,4,6-Trimethylphenoxy)benzonitrile

Into a 250 mL three-necked, round-bottomed flask equipped with a magnetic stir-bar, nitrogen inlet, and a condenser,

2,4,6-trimethylphenol (6.00 g, 44.1 mmol), 4-fluorobenzonitrile (5.34 g, 44.1 mmol), potassium carbonate (7.30 g, 52.8 mmol), and a mixture of NMP (100 mL) and toluene (60 mL) were placed. The reaction mixture was then heated and maintained around 140 °C for 8 h with vigorous nitrogen flow. The dark solution was filtered while it was warm and the filtrate was poured into distilled water containing 5% hydrochloric acid. The solution was separated into an organic layer and an aqueous layer. The organic layer was diluted with dichloromethane and separated. The solvent was removed to dryness. Light brown oily residue was freeze-dried to afford 10.1 g (97% yield): Anal. Calcd. for $C_{16}H_{15}NO$: C, 80.98%; H, 6.37%; N, 5.90%; O, 6.74%. Found: C, 80.31%; H, 6.37%; N, 5.75%; O, 6.46%. FT-IR (KBr, cm^{-1}): 2226 (C≡N stretch). Mass spectrum (*m/z*): 237 (M^+, 100% relative abundance), 222, 204, 194. ^1H NMR ($CDCl_3$, ppm) δ 2.05 (s, 6H, CH_3), 2.30 (s, 3H, CH_3), 6.81–6.84 (d, 2H, Ar), 6.91 (s, 2H, Ar), 7.53–7.56 (d, 2H, Ar). ^{13}C NMR ($CDCl_3$, ppm) δ 16.10, 20.79, 115.48, 129.07, 129.15, 129.88, 130.48, 134.25, 147.84, 150.03, 161.44.

2d. 4-(2,4,6-Trimethylphenoxy)benzoic acid

Into a 250 mL three-necked round-bottomed flask equipped with a magnetic stir-bar, nitrogen inlet, and a condenser, 4-(2,4,6-trimethylphenoxy)benzonitrile (10.0 g, 42.0 mmol) and phosphoric acid (100 mL) were placed. The reaction mixture was then heated and maintained around 150 °C for 8 h. After cooling down to room temperature, the mixture was poured into distilled water containing 5% hydrochloric acid. The resulting precipitates were collected by suction filtration, air-dried, dissolved in warm heptane, and filtered. The filtrate was allowed to cool to room temperature to afford 4.5 g (42% yield) of white crystal: mp 236–238 °C. Anal. Calcd. for $C_{16}H_{16}O_3$: C, 74.98%; H, 6.29%; O, 18.73%. Found: C, 74.76%; H, 6.67%; O, 18.56%. FT-IR (KBr, cm^{-1}): 1650 (C=O stretch), 3385 (O–H stretch). Mass spectrum (*m/z*): 256 (M^+, 100% relative abundance), 255. ^1H NMR (DMSO-d_6, ppm) δ 2.00 (s, 6H, CH_3), 2.67 (s, 3H, CH_3), 6.74–6.77 (d, 2H, Ar), 6.98 (s, 2H, Ar), 7.82–7.86 (d, 2H, Ar). ^{13}C NMR (DMSO-d_6, ppm) δ 15.80, 20.41, 113.80, 127.65, 129.69, 129.81, 130.12, 134.47, 147.95, 159.95, 167.06.

2e. Functionalization of VGCNF with 2,4,6-trimethylphenoxy)-benzoic acid

Into a 250 mL resin flask equipped with a high torque mechanical stirrer, and nitrogen inlet and outlet, 4-(2,4,6-trimethylphenoxy)benzoic acid (0.50 g, 1.95 mmol), VGCNF (0.50 g), and PPA (83% assay, 20 g) were placed and stirred with dried nitrogen purging at 130 °C for 3 h. P_2O_5 (5.0 g) was then added in one portion. The initially dark mixture became deep brown after 24 h. The temperature was maintained at 130 °C for 80 h. After cooling down to room temperature, water was added. The resulting precipitates were collected, washed with diluted ammonium hydroxide and Soxhlet extracted with water for three days and methanol for three days, and finally dried over phosphorus pentoxide under reduced pressure (0.05 mmHg) at 100 °C for 72 h to give 0.82 g (85% yield) of dark brown solid. Anal. Calcd. for $C_{148}H_{45}O_6$ (based on the assumption that for every 100 carbon, there are 3 2,4,6-trimethylphenoxybenzoyl groups attached): C, 92.63%; H, 2.36%; O, 5.00%. Found: C, 90.93%; H, 2.82%; O, 4.89%. [Calcd for VGCNT (C_∞): C, 100.00%; H, 0.00%; O, 0.00%. Found: C, 98.67%; H, 1.10%; O, <0.20% (less than detection limit)]. FT-IR (KBr, cm^{-1}): 1240, 1590, 1646, 2922, 3434.

3. Results and discussion

The diameter and length of the VGCNF (Pyrograf III-19-HT^{TM}) used in this work are in the ranges 100–200 nm and 30–100 μm, respectively. These VGCNF were heat-treated up to 3000 °C to graphitize the surface carbon and remove residual iron catalyst, and to improve the associated conducting properties. Since these vapor-grown carbon nanofibers (as opposed to carbon nanofibers from electro-spinning processes[9]) have hollow and concentric cores,[10] some researchers have considered them as MWNTs.[4,11] Although there are a number of reports in recent years on the utilization of as-received VGCNF in the development of thermoplastic, thermosetting and elastomeric nanocomposites,[10,12] there is still much room for improvement in the final composite properties. Aside from addressing the dispersion issues related to processing, enhancing the interfacial interections between the matrix material and the nanofibers should lead to greater improvement in the overall composite properties. Thus, it is expected that viable chemical modification of VGCNF surfaces, especially *via* solution chemistry, should provide means to improve the mechanical properties of VGCNF-based composites.

Previously, based on the model-compound studies, we found that the composition of the polyphosphoric acid and phosphorus pentoxide (PPA/P_2O_5) mixture is crucial to its effectiveness as a catalytic/dehydrative medium for the preparation of poly(ether-ketones). Thus, with the optimal weight ratio of 4 : 1 (PPA : P_2O_5), the Freidel–Crafts polycondensation of 3-phenoxybenzoic acid and related AB monomers was substantially promoted at 130 °C to yield the corresponding poly(ether-ketones) with significantly higher molecular weights.[13] More importantly, our study indicated that aryloxybenzoic acids formed acylium ions readily under our conditions. In conjunction with the observation that VGCNF dispersed rather well in PPA, we felt that the conditions might be conducive to a Friedel–Crafts acylation reaction between VGCNF and an appropriate aryloxybenzoic acid.

Thus, 4-(2,4,6-trimethylphenoxy)benzoic acid (TMPBA), **1**, was prepared in a two-step synthesis from postassium 2,4,6-trimethylphenolate and 4-fluorobenzonitrile, followed by treatment of the resulting nitrile intermediate with phosphoric acid. Apart from providing spectroscopic signatures useful for identification, the three methyl groups in **1** are strategically placed so as to block all positions activated by the aryl ether toward Friedel–Crafts acylation. The reaction of **1** and VGCNF in PPA/P_2O_5 was conducted according to the improved protocol that we reported previously (see Scheme 1).[13] The progress of the functionalization process was monitored by taking a small amount of aliquot at each time interval, 24, 38, 72, and 80 hours after the reaction temperature had been reached and kept constant at 130 °C. All aliquots were worked up the same way as the final product, and analysed with FT-IR (*vide infra*). Thus, after the reaction mixture had been precipitated in water, the crude product was washed with water, treated with aqueous ammonium hydroxide to neutralize the residual phosphoric acid and finally subjected to Soxhlet extraction with water for three days to completely remove residual phosphoric acid. For each sample, an additional Soxhlet extraction was conducted with methanol for three days to ensure the complete removal of any unreacted **1**. The resulting products were dried under reduced pressure (1 mmHg) at 100 °C for 72 h.

The analytical data are summarized in Table 1. It is noteworthy that the as-received VGCNF contains a significant amount of hydrogen (1.10 wt%), presumably attributable to the sp^3C–H and sp^2C–H defects as methane is used as the major component in the feedstock for the its production.[14] This is consistent with the fact that carbon nanotubes or nanofibers grown from chemical vapor processes (CVD) possess more defects on the surface in comparison with MWNTs from the arc-discharge method. Accordingly, the datum seems to suggest an upper limit that for every 8 carbon atoms, there is a hydrogen atom attached.

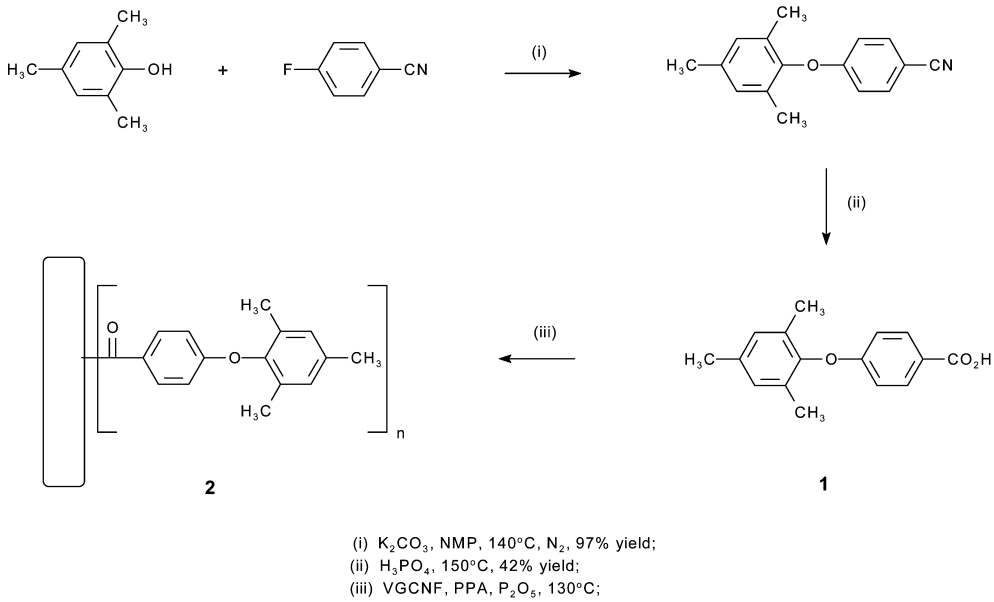

Scheme 1 Synthesis of 2,4,6-trimethylbenzoic acid and functionalization of VGCNF *via* Friedel–Crafts acylation.

Since the expected product should contain carbonyl groups, FT-infrared spectroscopy is a convenient yet informative analytical tool to monitor the progress and the extent of Friedel–Crafts acylation occurring on the VGCNF. The FT-IR spectra (KBr; the broad band at 3434 cm^{-1} is due to absorbed H_2O in KBr and can be used as a convenient reference) of the isolated products at reaction intervals of 24, 48, 72 and 80 h are shown in Fig. 1. It is apparent that under our conditions, the Friedel–Crafts acylation was relatively slow but progressing steadily as evidenced by the temporal growth of the aromatic ketone ν(CO) band at 1664 cm^{-1} as well as the characteristic stretches assignable to the methyl groups (2923 cm^{-1}) and Ar–O–Ar group (1232 cm^{-1}). Fig. 2 shows the comparative TGA behavior (in air and helium) of the original VGCNF and the functionalized VGCNF, **2**, isolated after 80 h of reaction. In air, the unmodified VGCNF underwent a catastrophic weight loss at temperatures >700 °C, but its major thermal degradation was delayed by *ca.* 50 °C in helium. In the case of **2**, we expected that the onset of weight loss under either air or helium atmosphere should commence at much lower temperatures because of the organic substituents. Indeed, in air the onset temperature of weight loss (38 wt%) occurred at 381 °C, attributable to the loss of arylcarbonyl substituents, and 62% of residue at 600 °C must be due to VGCNF. It is important to point out that the subsequent degradation pattern of the **2** is practically congruent with that of the unmodified VGCNF in the 600–850 °C region. Furthermore, it is noteworthy that at temperatures above 850 °C in helium atmosphere, the thermal stability of the modified VGCNF **2** appeared to be have been improved (*i.e.* lower weight loss) over the unmodified VGCNF. We speculate that such enhanced stability may arise from the homolytic fragmentation of the arylcarbonyl pendants from VGCNF, allowing the some skeletal rearrangements *via* free radical recombination processes toward more thermodynamically stable structures. Nevertheless, we believe that the basic molecular framework of VGCNF remained more or less intact during the Friedel–Crafts acylation in PPA. Based on the

Table 1 Elemental analysis data for functionalized VGCNF, **2**

Sample	Elemental Analysis	C (%)	H (%)	O (%)	P (%)
VGCNF	Calcd	100.00	0.00	0.00	0.00
	Found	98.87	1.10	<0.20[a]	<0.04[a]
Functionalized VGCNF	Calcd[b]	92.63	2.36	5.00	0.00
	Found	90.93	2.82	4.89	<0.08[a]

[a] Less than detection limit. [b] Calculated based on $C_{148}H_{45}O_6$, a proposed composition of **2** according to TGA (air) result.

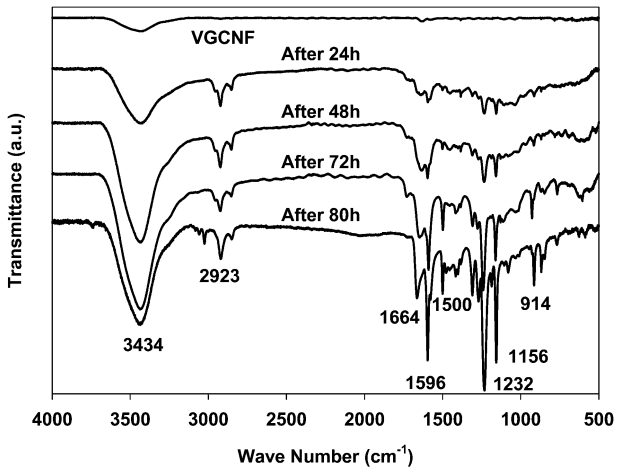

Fig. 1 FT-IR spectra showing the progress of Friedel–Crafts acylation reaction between VGCNF and 2,4,6-trimethylphenoxybenzoic acid in PPA at 130 °C.

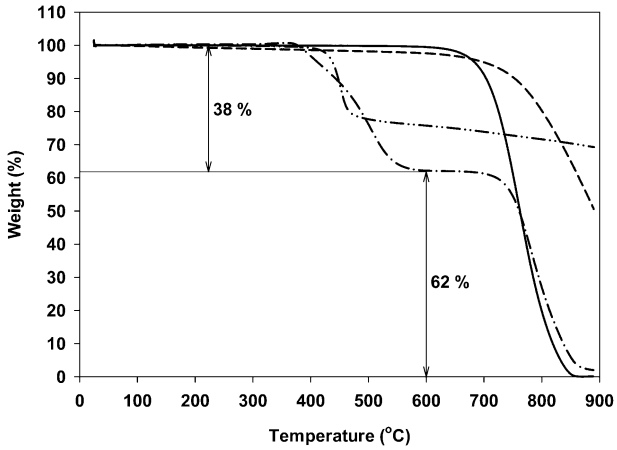

Fig. 2 TGA thermograms with heating rate of 10 °C min^{-1}: VGCNF in air (solid), VGCNF in helium (dash), **2** in air (dash-dot-dash), **2** in helium (dash-dot-dot-dash).

relative weight ratio of the substituents to VGCNF, it can be deduced that there are 3 arylcarbonyl groups covalently attached to the nanotube structure for every 100 carbon sites in contrast to a functionalization in every 20 carbons in the case of SWNT.[15] This is in accord with the expectation that SWNT should have more curvature strain (that drives the fullerene and CNT reaction chemistry) than VGCNF, since the diameters of the former are 1–2 orders of magnitude greater than the latter. In addition, we believe that the Friedel–Crafts reaction most probably takes placed at the sp^2C–H defect sites. In conjunction with the FT-IR results, we also believe that our acylation reaction conditions offer good control of the extent of functionalization to be imparted onto the VGCNF.

The functionalized VGCNF **2** is marginally soluble in aprotic amide solvents such as NMP, but appears to be more soluble in 1,2-dichlorobenzene. Two samples from an NMP solution were filtered through syringe filters with pore sizes of 0.45 and 1.0 μm. The filtrates were subjected to UV-vis absorption measurement and compared with **1** which absorbed intensely in the region 200–280 nm and showed an absorption cut-off around 350 nm (see Fig. 3). However, **2** displayed absorption maxima at 282 and 291 nm and its cut-off extends to ~500 nm, depending on the filter-pore size used. Apparently, when a filter with a larger pore size was used, more functionalized VGCNF were filtered through, leading to a general shift to higher absorption wavelength and intensity. The absorption maximum at 282 or 291 nm is tentatively assigned to the $\pi \rightarrow \pi^*$ transition associated with the conjugated C=O chromophore. The much weaker absorption tailing, ~350–500 nm, is assignable to the arylcarbonyl $n \rightarrow \pi^*$ transition.[16] This observation provides additional evidence for the covalent attachment of the arylcarbonyl moieties. Last but not least, scanning electron microscopy (SEM) revealed that the original VGCNF had smooth surfaces, but the surfaces of functionalized VGCNF are clearly decorated with covalently bonded moieties (see Fig. 4 and 5).

4. Conclusion

To our knowledge, we have demonstrated for the first time that Friedel–Crafts acylation in polyphosphoric acid is a viable, alternative route to effecting controlled functionalization of VGCNF. Our preliminary results also indicated the feasibility of grafting a poly(ether-ketone) onto VGCNF.[13] It is envisioned that the presence of versatile carbonyl functions on the carbon nanotubes will allow further development of application-specific derivatization chemistry to generate interesting VGCNF-based materials.

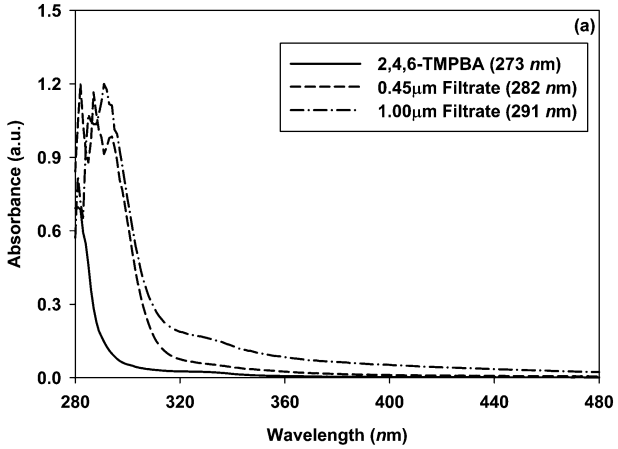

Fig. 3 UV-vis absorption spectra of 2,4,6-trimethylphenoxybenzoic acid and functionalized VGCNF **2** in NMP solutions filtered with membrane pore-size as indicated.

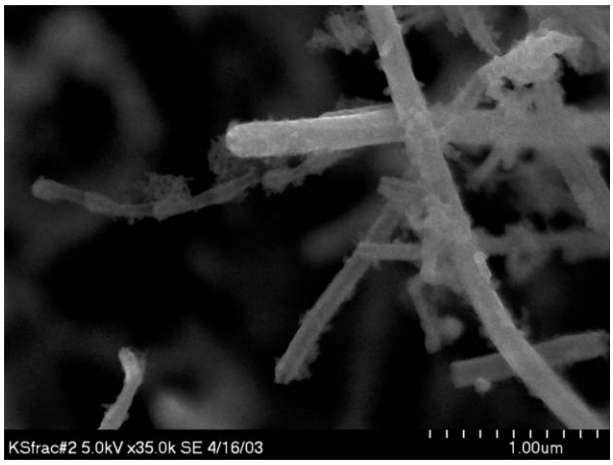

Fig. 4 SEM image of the functionalised VGCNF **2** at ×35000 magnification (Hitachi HRSEM 5200).

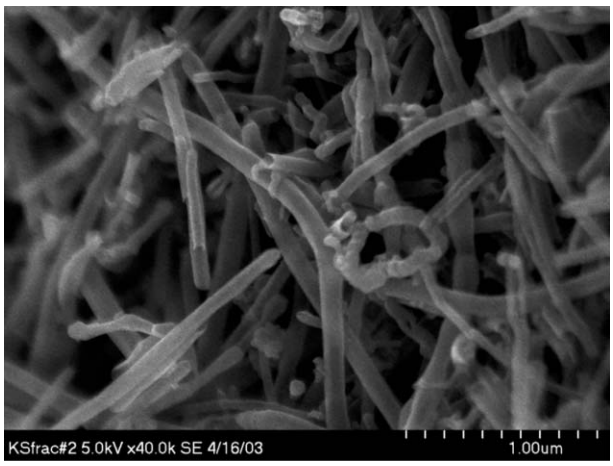

Fig. 5 SEM image of as-received VGCNF from Applied Sciences Inc. (at ×40000 magnification; Hitachi HRSEM 5200).

Acknowledgements

We are grateful to Marlene Houtz and Gary Price (both of University of Dayton Research Institute) for TGA data, and assistance in SEM imaging, and U.S. Air Force Office of Scientific Research for partial support of this work.

References

1 (*a*) B. Maruyama and A. Khairul, *SAMPE J.*, 2003, **38**(3), 59; (*b*) M. S. Dresselhaus, G. Dresselhaus and P. C. Eklund, *Science of fullerenes and carbon nanotubes*, Academic Press, San Diego, 1996.
2 M. M. J. Treacy, T. W. Ebbesen and J. M. Gibson, *Nature*, 1996, **381**, 678.
3 (*a*) D. Srivastava, C. Wei and K. Cho, *Appl. Mech. Rev.*, 2003, **56**, 215; (*b*) E. T. Thostenson, Z. Ren and T.-W. Chou, *Comp. Sci. Technol.*, 2001, **61**, 1899; (*c*) R. Andrews, D. Jacques, D. Qian and T. Rantell, *Acc. Chem. Res.*, 2002, **35**, 1008.
4 D. W. Schaefer, J. M. Brown, D. P. Anderson, J. Zhao, K. Chokalingam, D. Tomlin and J. Ilavsky, *J. Appl. Crystallogr.*, 2003, **36**, 553.
5 S. Kumar, T. Dang, F. E. Arnold, A. R. Bhattacharyya, B. G. Min, X. Zhang, R. A. Vaia, C. Park, W. W. Adams, R. H. Hauge, R. E. Smalley, S. Ramesh and P. A. Willis, *Macromolecules*, 2002, **35**, 9039.
6 For recent reviews: (*a*) Y.-P. Sun, K. Fu, Y. Lin and W. Huang, *Acc. Chem. Res.*, 2002, **35**, 1096; (*b*) V. N. Khabashesku, W. E. Billups and J. L. Margrave, *Acc. Chem. Res.*, 2002, **35**, 1087; (*c*) S. Niyogi, M. A. Hamon, H. Hu, B. Zhao, P. Bhowmik, R. Sen, M. E. Itkis and R. C. Haddon, *Acc. Chem. Res.*, 2002, **35**,

1105; (*d*) J. L. Bahr and J. M. Tour, *J. Mater. Chem.*, 2002, **12**, 1952.
7 N. Tagmatarchis, V. Georgakilas, M. Prato and H. Shinohara, *Chem. Commun.*, 2003, 2010.
8 http://www.apsci.com.
9 (*a*) Y. Wang, S. Serrano and J. J. Santiago-Aviles, *Synth. Met.*, 2003, **138**, 423; (*b*) C. Kim and K. S. Yang, *Appl. Phys. Lett.*, 2003, **83**, 1216; (*c*) Y. Wang, S. Serrano and J. J. Santiago-Aviles, *J. Mater. Sci. Lett.*, 2002, **21**, 1055.
10 For a TEM picture of "Pyrograf" nanofibers showing a bamboo-like structure, see P. Richard, T. Prasse, J. Y. Cavaille, L. Chazeau, C. Gauthier and J. Duchet, *Mater. Sci. Eng. A: Struct. Mater. Prop. Microstruct. Process.*, 2003, **A352**, 344.
11 (*a*) M. D. Alexander, Jr., H. J. Bentley and C.-S Wang, *Polym. Prepr. (Am. Chem. Soc., Div. Polym. Chem.)*, 2003, **44**(2), 294; (*b*) J. A. Stuckey, M. D. Alexander, Jr., B. M. Black and J. D. Henes, *Polym. Prepr. (Am. Chem. Soc., Div. Polym. Chem.)*, 2003, **44**(2), 141.
12 (*a*) J. Sandler, A. H. Windle, P. Werner, V. Altstaedt, M. V. Es and M. S. P. Shaffer, *J. Mater. Sci.*, 2003, **38**, 2135; (*b*) H. Ma, J. Zeng, M. L. Realff, S. Kumar and D. A. Schiraldi, *Polym. Mater. Sci. Eng.*, 2002, **86**, 411–412; (*c*) K. Lozano, J. Bonilla-Rios and E. V. Barrera, *J. Appl. Polym. Sci.*, 2001, **80**, 1162–1172; (*d*) K. Lozano and E. V. Barrera, *J. Appl. Polym. Sci.*, 2000, **79**, 125–133; (*e*) M. L. Lake, D. G. Glasgow, C. Kwag and D. J. Burton, *Int. SAMPE Symp. Exhib.*, 2002, **47**, 1794; (*f*) I. C. Finegan, G. G. Tibbetts, D. G. Glasgow, J. M. Ting and M. L. Lake, *J. Mater. Sci.*, 2003, **38**, 3485; (*g*) C. A. Cooper, D. Ravich, D. Lips, J. Mayer and H. D. Wagner, *Comp. Sci. Technol.*, 2002, **62**, 1105; (*h*) R. L. Jacobsen and D. G. Glasgow, *Proc. Am. Soc. Comp. Tech. Conf.*, 1999, **14**, 987.
13 J.-B. Baek and L.-S Tan, *Polymer*, 2003, **44**, 4135.
14 O. S. Carneiro, J. A. Covas, C. A. Bernardo, G. Caldeira, F. W. J. V. Hattum, J. M. Ting, R. L. Alig and M. L. Lake, *Comp. Sci. Technol.*, 1998, **58**, 401.
15 J. L. Bahr and J. M. Tour, *Chem. Mater.*, 2001, **13**, 3823.
16 C. N. R. Rao, *Ultra-violet and Visible Spectroscopy: Chemical Applications*, 2nd edn., Plenum Press, New York, 1967.